Chemical and Process Engineering 2021, 42 (1), 53–68
DOI: 10.24425/CPE.2021.137339

Modeling and simulation of an ideal plug flow reactor for synthesis of ethyl oleate using homogeneous acid catalyst

Suondos K.A. Barno[1], Sarmad A. Rashid[2], Ammar S. Abbas[2*]

[1]Presidency of the University of Baghdad, Baghdad, Iraq
[2]Chemical Engineering Department, College of Engineering, University of Baghdad, Baghdad, Iraq

The production of ethyl oleate, by homogenous acid esterification of oleic acid with ethanol, have discussed experimentally and via computational simulation in a plug flow reactor. An innovative simulation model has developed to predict the esterification reaction performance in an ideal plug flow reactor. The amount of H_2SO_4 acid catalyst, the initial molar ratio of alcohol to oleic acid, ethanol concentration, reaction temperature, and esterification time have examined their effects on ethyl oleate production and the conversion of oleic acid. Then the simulation extended to examine the esterification reaction kinetics and determine the reaction rate coefficients. The simulation results demonstrate that the increasing of H_2SO_4 acid, initial molar ratio of ethanol to oleic acid, ethanol concentration, and reaction temperature improved the productivity of the ethyl oleate and reduced the reactor space-time. The kinetics results illustrated that the reaction sensitivity to the temperature unchanging by using higher ethanol concentration and alcohol to oleic acid initial ratio. Lastly, the experimental yields at different conditions were slightly higher from those simulating with average values of 93.62 and 92.29%, respectively, indicating that the phenomenon of back-mixing cannot be ignored in esterification reactors, especially with a relatively high retention time within the reactor.

Keywords: kinetics, simulation, ethyl oleate, product distribution, back-mixing

1. INTRODUCTION

Ethyl oleate (EO) is a long-chain fatty acid ethyl ester formed by the reaction of the carboxy group of oleic acid (OA) with the hydroxy group of ethanol (EtOH) (Dan and Laposata, 1997). The key route of the production of EO is based on the esterification of free fatty acid with short chain alcohol over an acidic catalyst. Generally, the use of heterogeneous catalysts reduces the cost of biodiesel production, because of the ability of the reuse of the solid catalyst and minimize the cost of the separation steps of the products (Scragg, 2009). Esterification of OA with ethanol in the presence of catalytic acids has attracted a lot of attention, since the product EO can be used as a biodiesel (Gómez-Castro et al., 2016), solvents for the pharmaceutical industry, in the lipid modification (Bornscheuer, 2018), processing of Omega-3 oils (Hernandez 2011), and moreover, EO can serve as lubricant or plasticizer (Mod et al., 1977; Oliveira et al., 2010; Sena et. al, 2019).

Frequently, the most of the informed solid acid catalysts to esterify the OA with alcohols are; acid catalyst based on sulfated iron ore (Prates et al., 2020), amorphous carbon base (Liu et al., 2008; Takagaki et al., 2006), mesoporous tungsten trioxide (Sarkar et al., 2010), metal oxides (Refaat, 2011), zirconia (Oliveira et al., 2010), sulphated zirconia (Raia et al., 2017), tin (da Silva and Cardoso, 2013), pyridinium nitrate

* Corresponding author, e-mail: ammarabbas@coeng.uobaghdad.edu.iq

(Tankov and Yankova, 2019), hydroxyapatite (Chakraborty and Chowdhury, 2013), resin (Yin et al., 2012), montmorillonite-based clays (Bouguerra Neji et al., 2009), aluminum based catalysts (Al-Saadi et al., 2020; Gang and Wenhui, 2010), polypyrrole (Tang and Liang, 2015), metal organic frameworks (Chaemchuen et al., 2020; Zhou and Chaemchuen, 2017), zeolites with different acidity (Chung and Park, 2009), NaY (Abbas and Abbas, 2013a; 2015; Abbas et al., 2019), HY (Abbas et al., 2016; Alismaeel et al., 2018; Doyle et al., 2016; 2017), HZSM-5 (Alnaama, 2017; Majeed and Saleh, 2016; Vieira et al., 2015; Vieira et al., 2017), MCM-48 (Alfattal and Abbas, 2019) and 13X (Alshahidy and Abbas, 2020). Despite, the using of the heterogeneous catalysts, homogeneous catalysts are still used widely in the small processes of the esterification of OA to EO. Generally, esterification synthesis of EO is carried out between carboxylic acids (OA) and short chain alcohols (ethanol) with the presence of an acidic homogeneous catalyst (such as sulfuric acid, methane-sulfonic acid, phosphoric acid, trichloroacetic and hydrochloric acids) (Aranda et al., 2008; Beula and Sai, 2013; dos Santos et al., 2020) to form EO (ester) and water according to Eq. (1).

$$C_{18}H_{34}O_2 + C_2H_6O \xleftrightarrow{\text{Acid}(H^+)} C_{20}H_{38}O_2 + H_2O \tag{1}$$

The esterification step of fatty acids still has several practical challenges concerning the method of operation (batch or continuous). The key problem is water accumulation with the reaction proceed causing reducing the reaction speed and then less EO yield. To solve this issue, either reactive distillation column technology used or optimized the initial concentrations and reactor types and operating conditions (Higham, 2008; Karacan, 2015; Kiss and Bildea, 2012). Batch and plug flow reactors are usually used in the esterification reaction of OA. The choice of the plug flow reactor for the EO production was based on the fact that this reactor gives a higher yield than the mixed flow reactor for both homogeneous and heterogeneous catalysts (Abbas and Abbas, 2013b; 2013a; Alismaeel et al., 2018; Machado et al., 2015).

Here, we will report the simulation results of esterification synthesis of EO in an ideal flow plug flow reactor in details. Effects of the major process factors on the amount of the yield are going to be studying and discussing. These factors are the catalyst amount, initial ethanol to OA ratio, ethanol initial concentration, reaction temperature and reactor space-time. The work will study the reaction kinetics and discuss the product distribution, recommend the best operating conditions and then the research will be extended to make an extensive comparison between the simulating and experimental results.

2. SIMULATION MODEL AND EXPERIMENTAL WORK

2.1. Experimental data, model development and simulation algorithm

Esterification of OA with ethanol (EtOH) in presence of an acid catalyst (5 wt.% of H_2SO_4) produce EO and water (H_2O) (Eq. (1)). The reaction kinetics was found previously for the conversion of OA with commercial EtOH (88–90 wt.%) to produce EO (biodiesel) and water as a by-product in a temperature range between 40 and 70 °C, as in Eqs. (2) and (3) (Abbas and Abbas, 2013b).

$$-r_{OA} = k_1 C_{OA}^{n_1} C_{EtOH}^{m_1} - \frac{k_1}{K_{eq}} C_{EO}^{n_2} C_{H_2O}^{m_2} \tag{2}$$

$$K_{eq} = \frac{C_{EOe}^{n_2} C_{H_2Oe}^{m_2}}{C_{OAe}^{n_1} C_{EtOHe}^{m_1}} \tag{3}$$

The values of reaction orders, frequency factors and activation energies are listed in Table 1.

Table 1. Constants values of the reaction kinetics equation (Eq. 1) (Abbas and Abbas, 2013b)

Constant	k_{oeq}	E_{eq} [J/mol]	k_{o1}	E_1 [J/mol]	n_1	m_1	n_2	m_2
Value	$2.1{\cdot}10^7$	42189	196.3	26625	1.25	0.50	1.00	0.50

The conversion distribution of an limiting reactant (OA) over the plug flow reactor was calculated using the performance equation of an ideal plug flow reactor (Eq. 4) (Levenspiel, 1999).

$$\tau = \frac{V}{v_0} = \frac{VC_{\mathrm{OA}o}}{F_{\mathrm{OA}o}} = C_{\mathrm{OA}o}\int_0^{x_{\mathrm{OA}}} \frac{dx_{\mathrm{OA}}}{-r_{\mathrm{OA}}} \tag{4}$$

Concentrations of the reactants and products as a function of the conversion amount of OA (x_{OA}) (Eq. (5) to (8)) can be calculated according to the stoichiometric of Eq. (1).

$$C_{\mathrm{OA}} = C_{\mathrm{OA}o}\,(1 - x_{\mathrm{OA}}) \tag{5}$$

$$C_{\mathrm{EtOH}} = C_{\mathrm{EtOH}o} - x_{\mathrm{OA}}C_{\mathrm{OA}o} = C_{\mathrm{OA}}\,(M - x_{\mathrm{OA}}) \tag{6}$$

$$C_{\mathrm{EO}} = C_{\mathrm{EO}o} + x_{\mathrm{OA}}C_{\mathrm{OA}} \tag{7}$$

$$C_{\mathrm{H_2O}} = C_{(\mathrm{H_2O})o} + x_{\mathrm{OA}}C_{\mathrm{OA}o} \tag{8}$$

Finally, the yield of EO is calculated from in Eq. (9)

$$\text{EO yield, \%} = \frac{C_{\mathrm{EO}}}{C_{\mathrm{OA}o}} \times 100 \tag{9}$$

The pervious mathematical model was implemented using the programming language Python 3.8.2 (van Rossum, 1995). The solution algorithm of the model shown in Fig. 1.

2.2. Experimental work

The continuous esterification of OA with ethanol was performed in a vertical quartz plug flow reactor. The reactor has an internal diameter of 100 mm and height 650 mm connected with water-jacketed part (the internal diameter of jacket equal to 30 mm from each side of the reactor), the main elements for the continuous system are magnetic-heating stirrer for mixing and heating reactants and water bath used for supplying the heating water to the jacket to keep the reactor temperature at 70 °C. The calculated quantities of reactants are mixed and maintained at the 70 °C. As soon as the reactants have reached the desired temperature, H_2SO_4 catalyst and the reactants enter the reactor and flow upward with a chosen flow rate by two different dosing pumps. The product stream was collected in a gathering beaker, four samples of 5 mL were taken and centrifuged for 10 min at 3000 rpm to enhance the separation of organic phase (EO and unreacted OA) and the aqueous phase (EtOH and water). Four samples of 1 mL of the upper organic layer analysed by titration with 0.1 M KOH using phenolphthalein indicator, to calculate the acid value (AV) and then the OA conversion as shown in Eqs. (15) and (16) (Abbas and Abbas, 2013b; Abbas et al., 2016; Doyle et al., 2016). The average value obtained for OA conversion from the four samples were recorded and each experiment was repeated trice. Finally, the experimental EO yield was calculated from Eq. (10) and Eq. (11).

$$AV = \frac{\text{mL of KOH} \times N \times 56.1}{\text{weight of sample}} \tag{10}$$

$$x_{\mathrm{OA}},\ \% = \frac{AV_{t0} - AV_t}{AV_{t0}} \times 100 \tag{11}$$

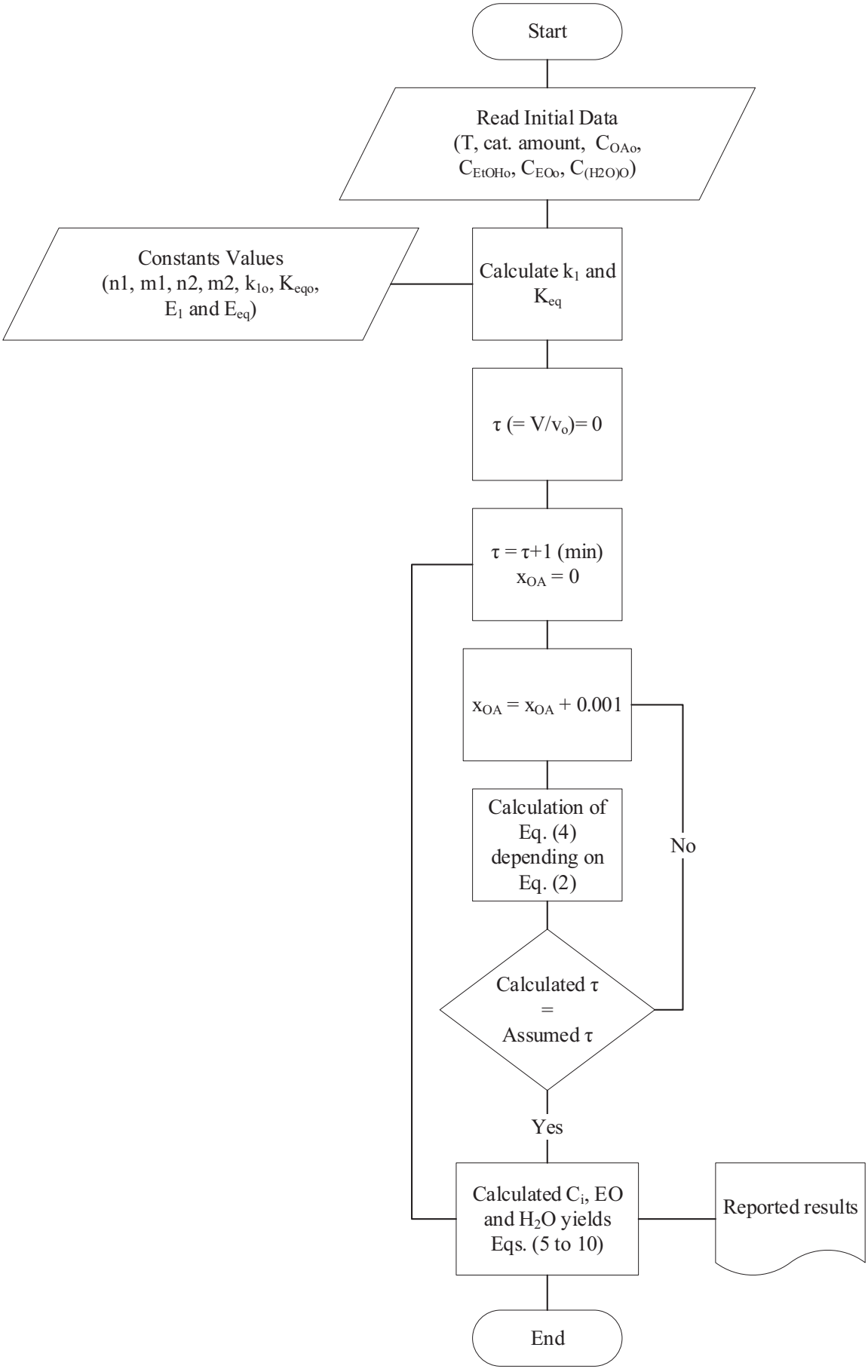

Fig. 1. Model solution algorithm by Python

3. RESULTS AND DISCUSSION

3.1. Effect of catalyst amount on the EO yield

The effect of the amount of catalyst based on the initial amounts of OA initial (1 to 5 wt.%) was simulated at esterification temperature of 70 °C, 6/1 ethanol to OA ratio, with EtOH concentration of 90%. As shown in Fig. 2, the esterification reaction increased significantly with catalyst amount for the same space-time. For 100 min space-time, the EO yield was only about 18% when 1 wt.% catalyst amount was used, while the EO yield was 86% when 5 wt.% of the catalyst was applied. Thus, higher catalyst ratio gives higher EO yield in shorter space-time (smaller reactor for the same flow rate). The EO yield required 71 of minutes space-time to reach the EO equal to 60% when using 4 wt.% catalyst versus 12.5 min of space-time when 5 wt.% of catalyst used. So, for the same flow rate (production rate), smaller reactor volume is required when higher catalyst to OA ratio utilized. For the space-time 150 min and more, no significant change is noticed for the catalyst amounts 1 and 2 wt.%, while for the catalyst amounts of 3, 4 and 5 wt.%, the EO yield changes slowly with the increasing reactor space-time.

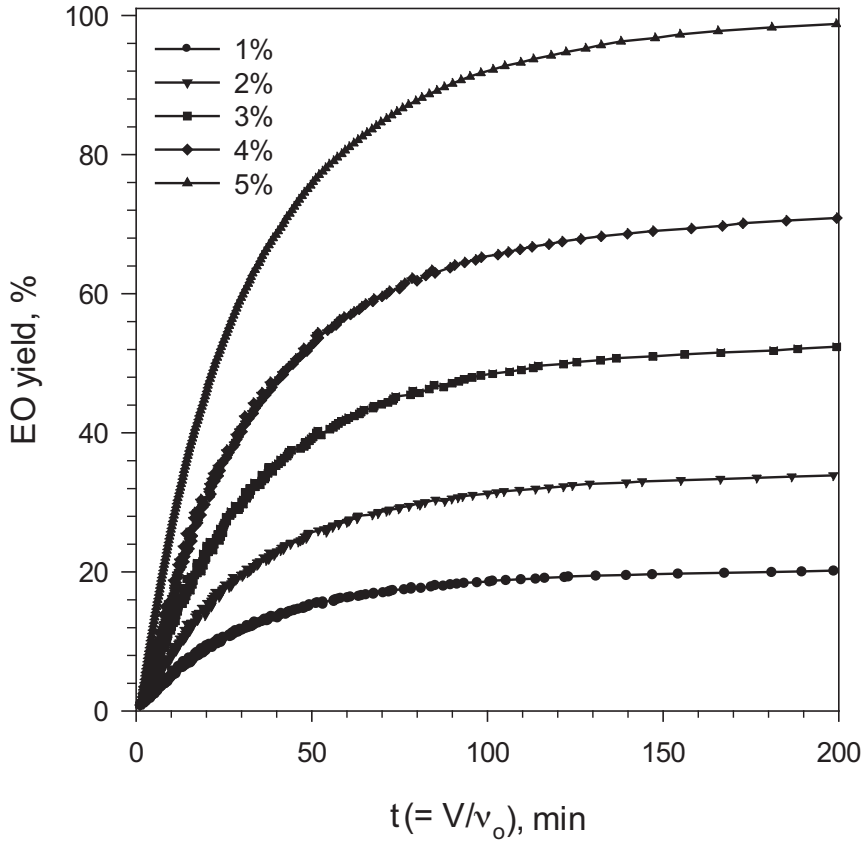

Fig. 2. Space-time versus EO yield at different catalyst amounts at 70 °C and 6/1 of 90 wt.% of EtOH to OA

The initial step of esterification reaction carried out between OA (free fatty acid) and EtOH (short chain alcohol) was protonation of the acid to give an oxonium ion (H_3O^+) (Khan 2002), as higher acid ratio is used, a higher number of H^+ ions will appear in the reactant mixture, therefore the reaction rate increases because of the increasing H_3O^+ formed and then increasing the possibility to initiate the esterification reaction, promote the exchange reaction between carboxylic acids (free fatty acids) and alcohols to produce ester.

3.2. Effect of M and ethanol concentration on the EO yield and water produced

Esterification of OA with EtOH is a reversible reaction with a stoichiometry ethanol/oil molar ratio of 1:1. Usually, an excess amount of ethanol is used to obtain better EO yield. Table 2 summarized the EO yield versus different initial EtOH/OA molar ratio (M) using different ethanol concentration, at 70 °C, V/ν_o = 150 min and 5% cat. amount. From Table 2 and for each EtOH concentration, the EO yield increased proportionally with the M increase, and it can be realized that noteworthy increase of EO yield when the M increase from 3/1 to 6/1 is observed, while a further increase in M from 6/1 to 9/1 does not significant enhanced EO yield. Likewise, increasing EtOH concentration rises slightly the EO yield (Table 2), and produces less water content to each mole of OA feed, as shown in Table 3. Otherwise, using lower EtOH concentration and higher M, means using more water in the feed, so the product will contain more water. The presence of more water in the product will cause the subsequent separation cost to rise.

Table 2. EO yield versus initial molar ratio at different ethanol concentration, temperature 70 °C, V/ν_o = 150 min and 5% cat. amounts

	EO yield,%		
M	90% wt. ethanol	95% wt. ethanol	100% wt. ethanol
3/1	90.51	92.32	93.58
6/1	96.26	96.59	97.37
9/1	97.56	97.89	98.35

Table 3. Water mole produced for one mole OA at different ethanol concentration, temperature 70 °C, V/ν_o = 150 min and 5% cat. amounts

	H_2O produce/OA feed (mol/mol)		
M	90% wt. ethanol	95% wt. ethanol	100% wt. ethanol
3/1	1.5686	1.2789	0.9358
6/1	2.2895	1.6772	0.9737
9/1	2.9660	2.0459	0.9835

Generally, the mechanism of the esterification involves one mole of the triglyceride needed to react with one mole of the alcohol (Eq. (1)), but this ratio is not applied practically since the reaction is reversible. Therefore, an excess amount of alcohol is used for shifting the equilibrium of the reaction towards the product formation and reduce the effect of the backward reaction. High value of M may largely increase the water content in the reaction mixture causes slowing esterification and accordingly reduces the yield of the direct reaction. Consequently, unreacted alcohol must be recycled for reuse and an enormous amount of energy is needed. Hence, cost-effective optimal values of M and EtOH concentration are to be determined as the best probable of separation energy saving.

3.3. Effect of reactor temperature and space-time on EO yield

The reaction temperature has an important consideration on the kinetics of reactions, because the temperature affects temperature-dependent coefficient (reaction rate constant) according to Arrhenius's law. Fig. 3 shows the EO yield against the reactor space-time at different temperatures (40, 50, 60 and 70 °C) using 100 wt.% of EtOH with M equal to 9/1 and 5 wt.% H_2SO_4 relative to OA. These values (EtOH

concentration, M, and catalyst amount) were selected because they give better EO yield. It is clearly in Fig. 3 that EO yield increase with increasing temperature and reactor space-time. As the temperature increased both the yield and the speed of the reaction improved. For instance, the EO yield at 40 °C is about 63% using reactor space-time of 60 min, while the yield was enhanced to 89% at 70 °C. As the reaction speed improved with temperature, less reactor space-time (less reactor volume for the same flow rate) was required to achieve same conversion, noticing, it was required only 22.7 min at 70 °C to achieve 63% yield versus 60 min when 40 °C used. Generally, the higher temperature (70 °C) gives better yield with less reactor space-time, and the high yield of 96% does not change dramatically for the reactor space-time greater than 100 min These results are expected and in agreement with previous works for esterification of OA with EtOH using homogeneous catalyst (Abbas and Abbas, 2013b; 2016), since the increase in temperature leads to increase in molecular activity and rise the probability of molecules to react causing boost in reaction rate constant according to the collusion theory and Arrhenius law (Froment et al., 2011; Harriott, 2002; Levenspiel, 1999; Mann, 2009).

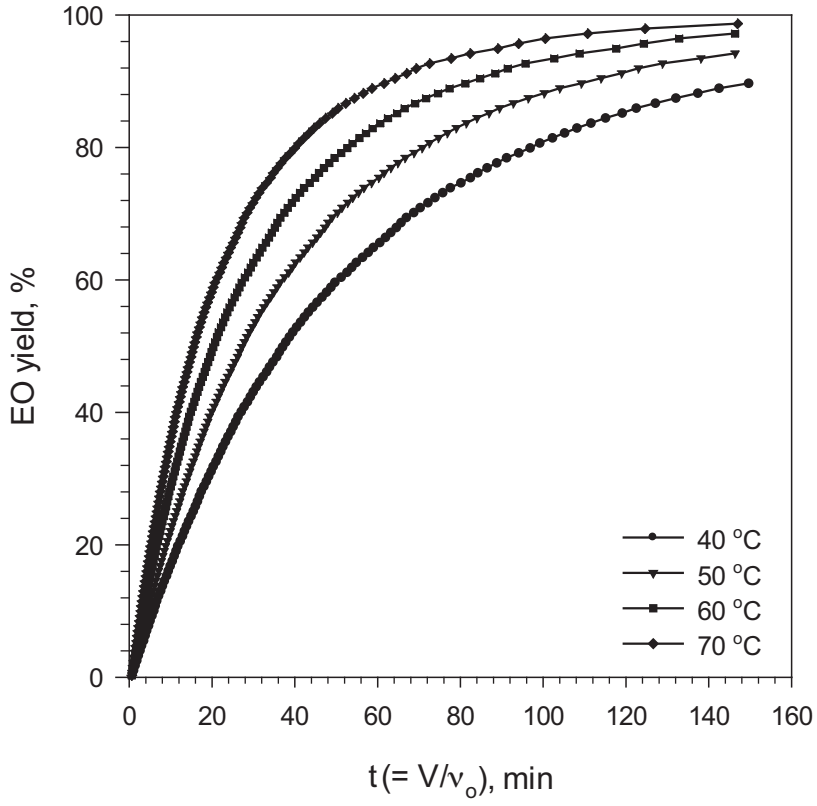

Fig. 3. Space-time versus EO yield at different catalyst amounts at 70 °C and 9/1 of 100 wt.% of EtOH to OA and 5% catalyst amounts

3.4. Kinetics of the OA consumption using fractional-life method

Fractional-life method (Levenspiel, 1999) was used to determine the kinetics equation that described the OA consumption at 70 °C, 9/1 of pure EtOH to OA and 5 wt.% catalyst amounts. When the higher M (9/1) is used, the forward reaction becomes more dominance and the backward reaction fades away. The reaction rate equation for the consumption of the reactants can be written according to Eq. (1) as:

$$-r_{\mathrm{OA}} = k\, C_{\mathrm{OA}}^{\alpha}\, C_{\mathrm{EtOH}}^{\beta} \tag{12}$$

For high M (9/1), Eq. (12) becomes

$$-r_{\mathrm{OA}} = \left[k\,(C_{\mathrm{EtOH}})_o^{\beta}\right] C_{\mathrm{OA}}^{\alpha} \tag{13}$$

$$-r_{\mathrm{OA}} = k' C_{\mathrm{OA}}^{\alpha} \tag{14}$$

where:

$$k' = k\,(C_{\mathrm{EtOH}o})_o^{\beta} \tag{15}$$

$$-r_{\mathrm{OA}} = -\frac{dC_{\mathrm{OA}}}{dt} = k' C_{\mathrm{OA}}^{\alpha} \tag{16}$$

Integrating Eq. (21), gives:

$$C_{\mathrm{OA}}^{1-\alpha} - C_{\mathrm{OA}o}^{1-\alpha} = k'(\alpha - 1)t \tag{17}$$

Defining the fractional lifetime of the reaction, τ_F, as the space-time necessary for the concentration of reactants to drop to fractional (*Frac*) of the initial concentration $C_{\mathrm{OA}o}$. Equation (17) can be written as:

$$\tau_{Frac} = \frac{Frac^{1-\alpha} - 1}{k'(\alpha - 1)} C_{\mathrm{OA}}^{1-\alpha} \tag{18}$$

$$\ln(\tau_{Frac}) = \ln\left(\frac{Frac^{1-\alpha} - 1}{k'(\alpha - 1)}\right) + (1 - \alpha)\ln(C_{\mathrm{OA}o}) \tag{19}$$

Use the fractional-life method with *Frac* ($C_{\mathrm{OA}}/C_{\mathrm{OA}o}$) = 90%. The data of fractional lifetime for different initial conditions (concentration of OA at 9/1 of 100 wt.% of EtOH to OA and 5 wt.% catalyst amounts) was summarized in Table 4, and a plot of Eq. (24) with the data of Table 4 is shown in Fig. 4.

Table 4. Fractional-life space-time for different initial concentration of OA at different temperatures, 9/1 of 100 wt.% of EtOH to OA, and 5% cat. amounts

	Fractional-life space-time [min]			
Initial OA concentration [mol/l]	40 °C	50 °C	60 °C	70 °C
1.00	5.41	3.82	2.88	2.21
0.90	5.45	4.04	3.01	2.32
0.80	5.58	4.1	3.12	2.43
0.70	5.63	4.41	3.24	2.51
0.60	6.55	4.65	3.33	2.61

The obtained slopes, $(1-\alpha)$, the intercepts $\ln\left(Frac^{1-\alpha} - 1/k'\,(\alpha - 1)\right)$, the average reaction order and the reaction rate constants at the various temperatures are summarized in Table 5. The activation energy can be calculated from the reaction rate constant according to the Arrhenius's equation (Eq. (20)) (Levenspiel, 1999). The activation energy and pre-exponential factor can be calculated by converting the Arrhenius's equation to the linear form for a specific range of temperatures as Eq. (21).

$$k' = k'_o e^{\frac{-E}{RT}} \tag{20}$$

$$\ln k' = \ln k'_o - \left(\frac{E}{R}\right)\frac{1}{T} \tag{21}$$

The linear form (Eq. (21)) of the Arrhenius equation was plotted in Fig. 5.

The calculated activation energy for the esterification reaction was 26.145 kJ/mole and the frequency factor is 462.25 in the temperature range from 40 to 70 °C. The obtained value of the reaction order with respect to OA (1.31) and the activation energy were in the same magnitudes of the reaction order with respect to OA and activation energy of the experimental data with those found for M = 6/1 and 90% wt. ethanol (1.25 and 26.625 kJ/mole, respectively). Whereas, the value of the obtained frequency factor was higher than the reported previously (196.3) (Abbas and Abbas, 2013b). Thus, the esterification reaction sensitivity to change in concentration and temperatures does not affect using higher M and pure ethanol, but with higher reaction rate constant because of the higher value of the obtained frequency factor.

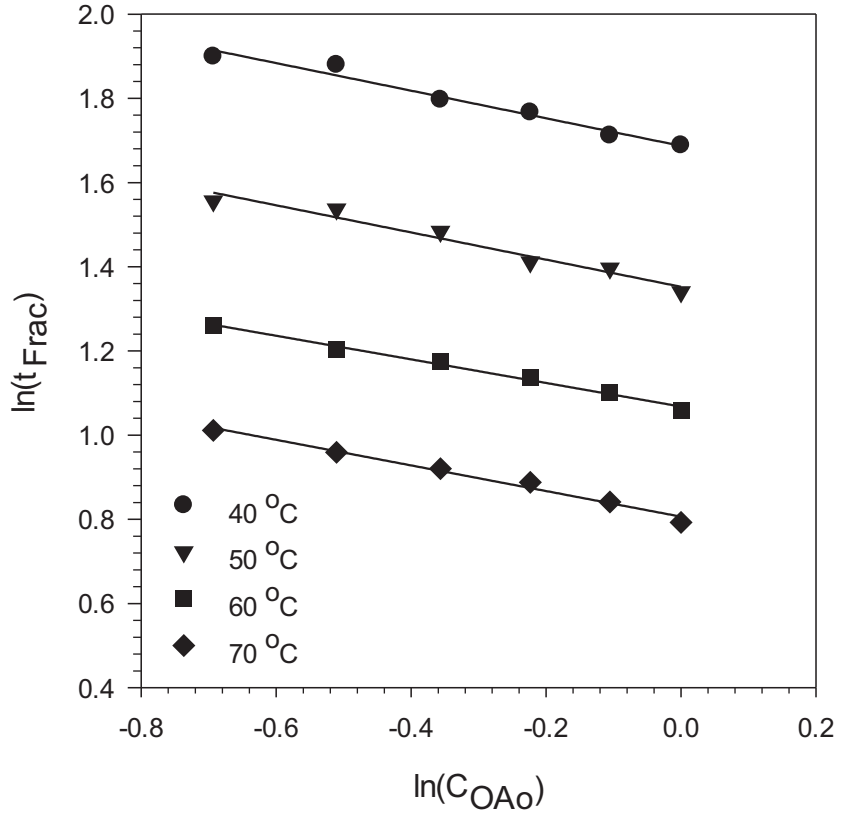

Fig. 4. Plot of Eq. (19) at reaction temperatures, for 9/1 of 100 wt.% of EtOH to OA and 5 wt.% catalyst amounts

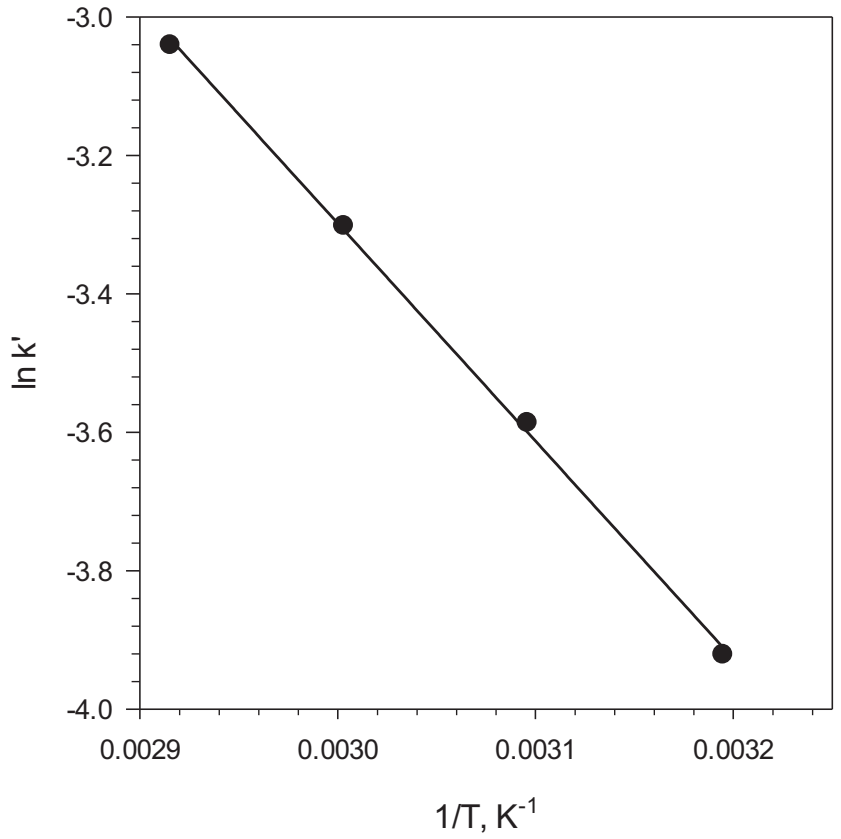

Fig. 5. Arrhenius plot of the obtained reaction rate constants versus different temperatures, for 9/1 of 100 wt.% of EtOH to OA, and 5% catalyst amounts

Table 5. Slopes and intercepts of Eq. (17), the obtained reaction order and the values of reaction rate constants (k') at different temperatures, 9/1 of 100 wt.% of EtOH to OA, and 5% cat. amounts

	40 °C	50 °C	60 °C	70 °C
Slope (1-α)	–0.3276	–0.3225	–0.2802	–0.3040
Intercept	1.6872	1.3525	1.0680	0.8066
Reaction order (average α)	1.31			
k', $(\text{mol/l})^{-0.31}(\text{min})^{-1}$	0.01982	0.02770	0.03681	0.04781

3.5. Reactor space-time and products distributions

The reactor space-time required for definite yields (90 to 98%) were calculated and organized in Table 6, for different M and EtOH concentrations at 70 °C and 5% cat. amounts. As expected, higher yield required more space-time for specific M and alcohol concentration. Whereas, for a certain yield, rising M and/or EtOH concentration minimized the reactor space-time. Also, Table 6 shows that M is highly affected on reducing the reactor space-time than on the alcohol concentrations, and this effect decreases with the increasing of EO yield. The previous studies (Abbas and Abbas, 2013b; 2016) reported a time of about 90 min for 92% of OA conversion, using 6/1 ethanol to OA ratio in a batch reactor while the required space-time ranged between 88.4 to 102.1 min for 92% of EO yield in the simulated results for the plug flow reactor. Thus, for the 92% EO yield, the increasing of M to 9 with the same EtOH concentrations (90 to 100 wt.%) enables reducing the reactor space-time by 18–20 min (to the range of 70.3 to 83.4 min). This change in reactor space-time will diminish reactor size by about 20% or improve the reactor productivity (enhance the volumetric flow rate).

Table 6. Reactor space-time ($\tau = V/\nu_o$) for different M and ethanol concentration, temperature 70 °C and 5% cat. amounts

		τ, min		
EO yield,%	M	90% wt. ethanol	95% wt. ethanol	100% wt. ethanol
90.0	3/1	145.4	128.1	116.5
	6/1	96.3	85.0	79.2
	9/1	74.9	71.6	63.5
92.0	3/1	165.8	145.3	133.8
	6/1	102.1	94.8	88.4
	9/1	83.4	81.3	70.3
94.0	3/1	196.1	173.2	156.6
	6/1	118.1	105.4	103.1
	9/1	98.7	93.3	85.2
96.0	3/1	235.4	213.9	191.5
	6/1	148.3	138.5	126.5
	9/1	125.1	111.6	99.8
98.0	3/1	319.5	281.1	257.1
	6/1	206.1	188.3	165.8
	9/1	180.9	153.6	135.3

EO yield of 94% produced using reactor space-time less than 100 min only with M equal to 9 for all studied alcohol's concentrations. 96% of EO yields in 99.8 min of reactor space-time for M equal to 9 and using pure ethanol. Yield of 98% of EO needs reactor space-time greater than 100 min. While lower EO yield (90%) needs at least 63 minutes' space-time when higher M and ethanol concentration used. The recommended higher yield with a suitable reactor space-time (99.8 min) was 96% that produced using M of 9 and pure ethanol.

3.6. Experimental esterification results

The EO yield values which obtained from the experimentally measured values of OA conversion were verified and compared with the simulated results, at a selected range of the reactor space-time (120 min and less), ethanol to OA initial molar ratio, and the ethanol concentration for the highest reaction temperature and catalyst load, as shown in Table 7. All values of experimental EO yield results were higher than their counterparts obtained from the simulation process. The average experimental EO yield (93.62%) was

Table 7. Experimental versus simulated measured OA conversion and EO yield

M	EtOH conc. [%]	τ [min]	Simulated EO yield [%]	Experimental EO yield [%]
3/1	100	116.5	90	92.3
6/1	90	96.3	90	92.5
6/1	95	85.0	90	92.1
6/1	100	79.2	90	91.8
9/1	90	74.9	90	92.4
9/1	95	71.6	90	92.2
9/1	100	63.5	90	92.1
6/1	90	102.1	92	93.6
6/1	95	94.8	92	93.5
6/1	100	88.4	92	93.3
9/1	90	83.4	92	93.2
9/1	95	81.3	92	93.1
9/1	100	70.9	92	92.9
6/1	90	118.1	94	95.2
6/1	95	105.4	94	94.9
6/1	100	103.1	94	94.7
9/1	90	98.7	94	94.5
9/1	95	93.3	94	94.4
9/1	100	85.2	94	94.3
9/1	95	116.6	96	96.6
9/1	100	99.8	96	96.4
Arithmetic mean			92.29	93.62
Average error [%]			1.46	
Average Deviation [%]			1.24	

higher the simulated values of EO yield (92.29%), with the average error and deviation of 1.46% and 1.24%, respectively.

The differences between experimental and simulating results reduce with the increase in the esterification yield and the decrease in space-time of the reactor. Perhaps the process of understanding this phenomenon requires an in-depth study to include variables such as the amount of reacted and product materials, reaction kinetics, temperature, the physical properties of the materials and the geometry of the reactor (Gültekin S. and Kalbekov, 2017). But it can provide a preliminary explanation these rising values of experimental EO yield by using the non-ideal flow phenomenon hypothesis, which occurs in real reactors. The back-mixing, dead zone, vortex formation and sluggish behavior possibly increase with increasing space-time of the reactor causes an irregular residence time distribution of the materials in the reactor and tends toward delay the reactants more time than designed (Levenspiel and Bischoff, 1959; Levenspiel, 1999; Harriott, 2002).

4. CONCLUSIONS

Despite challenges, the model for esterification reaction has been established for carrying out the simulation of the esterification of OA and ethanol catalysed homogeneously by H_2SO_4 using the previously published data (Abbas and Abbas, 2013b). Simulating results describes a positive effect of increasing the amount of catalyst on the enhancing of the EO yield and reducing of the reactor space-time, because of H_3O^+ ion increase in the reaction mixture. Higher concentrations of alcohol improved the yield and reduce the reactor space-time and produces less water in the product, which decrease the cost of the subsequent separation process of the products. Using higher M in the esterification reaction, not only improves the amount of the EO yield and reduces the reactor volume for the same productivity, but also enhances the forward reaction rate, and ended the reverse reaction. The study of the reaction kinetics using the fractional-life method, which is based on the hypothesis that the forward reaction is the main dominant and the absence of a backward reaction when using the highest value of M (1/1), reviled that the values of the reaction constant are higher than the values of the previous results (Abbas and Abbas, 2013b) due to the initial higher concentration and ratio of alcohol used while the reaction degree and activation energy values did not change much, which confirms that the reaction kinetics response to the change in concentration while its sensitivity to temperature remains unchanged. In general, increasing the reaction temperature increases the value of the EO yield and improves the rate of the reaction, thereby reducing the size of the reactor. Simulation of reactor operation in extreme conditions reduced the reactor space-time by 20%. Finally, laboratory results of producing EO were better than those obtained from the simulation at the same conditions, which indicates that the phenomenon of back-mixing has a pronounced effect in delaying the materials within the reactor resulting in increase of the retention time more than required. Thus, it is advisable to study this phenomenon and the factors affecting it such as the geometry of the reactor, the variation in the physical properties of the materials and the reaction kinetics.

SYMBOLS

C	concentration, mol/m^3
E	activation energy, J/mol
F	molar rate, mol/min
$Frac$	fractional-life, min
K	equilibrium constant, –
k	reaction rate constant, 1/min
M	initial molar ratio

r	reaction rate, mol/(m^3·min)
R	universal gas constant, 8.314 J/(mol·K)
T	temperature, K
V	reactor volume, m^3
x	conversion, –

Greek symbols

α	OA reaction order
β	ethanol reaction order
ν	volumetric flow rate, m^3/min
τ	reactor space-time, min

Superscripts

n, m	reaction orders

Subscripts

1	forward reaction
2	backword reaction
EO	ethyl oleate
eq	equilibrium
EtOH	ethanol
f	final
Frac	fraction-time
H_2O	water
o	initial
OA	oleic acid

REFERENCES

Abbas A.S., Abbas R.N., 2013a. Kinetic study and simulation of oleic acid esterification over prepared NaY zeolite catalyst. *Iraqi J. Chem. Pet. Eng.* 14 (4), 35–43.

Abbas A.S., Abbas S.M., 2013b. Kinetic study and simulation of oleic acid esterification in different type of reactors. *Iraqi J. Chem. Pet. Eng.* 14 (2), 13–20.

Abbas A.S., Abbas S.M., 2016. Giresun Taguchi experimental design, optimization and kinetic study of biodiesel production from oleic acid, *X^{th} International Statistics Days Conference*. Giresun University, Giresun, 743–754.

Abbas A.S., Albayati T.M., Alismaeel Z.T., Doyle, A.M., 2016. Kinetics and mass transfer study of oleic acid esterification over prepared nanoporous HY zeolite. *Iraqi J. Chem. Pet. Eng.*, 17 (1), 47–60.

Abbas A.S., Hussein M.Y., Mohammed H.J., 2019. Preparation of solid catalyst suitable for biodiesel production. *Plant Arch.*, 19 (2), 3853–3861.

Abbas A.S., Abbas R.N., 2015. Preparation and characterization of NaY zeolite for biodiesel production. *Iraqi J. Chem. Pet. Eng.*, 16 (2), 19–29.

Alfattal A.H., Abbas A.S., 2019. Synthesized 2nd generation zeolite as an acid-catalyst for esterification reaction. *Iraqi J. Chem. Pet. Eng.* 20 (3), 67–73. DOI: 10.31699/IJCPE.2019.3.9.

Alismaeel Z.T., Abbas A.S., Albayati T.M., Doyle A.M., 2018. Biodiesel from batch and continuous oleic acid esterification using zeolite catalysts. *Fuel*, 234, 170–176. DOI: 10.1016/j.fuel.2018.07.025.

Alnaama A.A., 2017. Synthesis and characteriazation of nanacrystalline ZSM-5 and ZSM-5/MCM-41 composite zeolite for biodiesel production. *Ph.D. Thesis*, *University of Baghdad*.

Al-Saadi A., Mathan B., He Y., 2020. Esterification and transesterification over SrO- ZnO/Al_2O_3 as a novel bifunctional catalyst for biodiesel production. *Renew. Energy*, 158, 388–399. DOI: 10.1016/j.renene.2020.05.171.

Alshahidy B.A., Abbas A.S., 2020. Preparation and modification of 13X zeolite as a heterogeneous catalyst for esterification of oleic acid. *AIP Conference Proceedings*, 2213, 020167. DOI: 10.1063/5.0000171.

Aranda D.A.G., Santos R.T.P., Tapanes N.C.O., Ramos A.L.D., Antunes O.A.C., 2008. Acid-catalyzed homogeneous esterification reaction for biodiesel production from palm fatty acids. *Catal. Lett.* 122, 20–25. DOI: 10.1007/s10562-007-9318-z.

Beula C., Sai P.S.T., 2013. Kinetics of esterification of palmitic acid with ethanol- optimization using statistical design of experiments. *Int. J. Chem. Eng. Appl.* 4, 388–392. DOI: 10.7763/ijcea.2013.v4.331.

Bornscheuer U., 2018. *Lipid modification by enzymes and engineered microbes*. Elsevier Inc. DOI: 10.1016/c2016-0-04104-9.

Bouguerra Neji S., Trabelsi M., Frikha M.H., 2009. Esterification of fatty acids with short-chain alcohols over commercial acid clays in a semi-continuous reactor. *Energies* 2, 1107–1117. DOI: 10.3390/en20401107.

Chaemchuen S., Heynderickx P.M., Verpoort F., 2020. Kinetic modeling of oleic acid esterification with UiO-66: from intrinsic experimental data to kinetics via elementary reaction steps. *Chem. Eng. J.* 394, 124816. DOI: 10.1016/j.cej.2020.124816.

Chakraborty R., Chowdhury R.D., 2013. Fish bone derived natural hydroxyapatite-supported copper acid catalyst: Taguchi optimization of semibatch oleic acid esterification. *Chem. Eng. J.* 215–216, 491–499. DOI: 10.1016/j.cej.2012.11.064.

Chung K.H., Park B.G., 2009. Esterification of oleic acid in soybean oil on zeolite catalysts with different acidity. *J. Ind. Eng. Chem.*, 15, 388–392. DOI: 10.1016/j.jiec.2008.11.012.

da Silva M.J., Cardoso A.L., 2013. Heterogeneous tin catalysts applied to the esterification and transesterification reactions. *J. Catal.* 2013, 1–11. DOI: 10.1155/2013/510509.

Dan L., Laposata M., 1997. Ethyl palmitate and ethyl oleate are the predominant fatty acid ethyl esters in the blood after ethanol ingestion and their synthesis is differentially influenced by the extracellular concentrations of their corresponding fatty acids. *Alcohol.: Clin. Exp. Res.*, 21, 286–292. DOI: 10.1111/j.1530-0277.1997.tb03762.x.

dos Santos R.C.M., Gurgel P.C., Pereira N.S., Breves R.A., de Matos P.R.R., Silva L.P., Sales M.J.A., Lopes R. de V.V., 2020. Ethyl esters obtained from pequi and macaúba oils by transesterification with homogeneous acid catalysis. *Fuel* 259, 116206. DOI: 10.1016/j.fuel.2019.116206.

Doyle A.M., Albayati T.M., Abbas A.S., Alismaeel Z.T., 2016. Biodiesel production by esterification of oleic acid over zeolite Y prepared from kaolin. *Renewable Energy*, 97, 19–23. DOI: 10.1016/j.renene.2016.05.067.

Doyle A.M., Alismaeel Z.T., Albayati T.M., Abbas A.S., 2017. High purity FAU-type zeolite catalysts from shale rock for biodiesel production. *Fuel*, 199, 394–402. DOI: 10.1016/j.fuel.2017.02.098.

Froment G.F., Bischoff K.B., De Wilde J., 2011. *Chemical reactor analysis and design*. 3^{rd} ed. John Wiley & Sons, Inc.

Gang L., Wenhui P., 2010. Esterifications of carboxylic acids and alcohols catalyzed by $Al_2(SO_4)_3$•$18H_2O$ under solvent-free condition. *Kinet. Catal.* 51, 559–565. DOI: 10.1134/S0023158410040154.

Gómez-Castro F.I., Gutiérrez-Antonio C., Romero-Izquiero A.G., Morales-Rodríguez R., Segovia-Hernández J.G., 2016. Mass and energy integration for the supercritical process for biodiesel production and a bioethanol dehydration train. *Comput. Aided Chem. Eng.*, 38, 487–492. DOI: 10.1016/B978-0-444-63428-3.50086-2.

Gültekin S., Kalbekov A., 2017. Effect of back mixing on the performance of tubular-flow reactors. *Int. J. Dev. Res.*, 7 (9), 15684–15685.

Harriott P., 2002. *Chemical reactor design*. CRC Press, New York. DOI: 10.1201/9780203910238.

Hernandez E.M., 2011. Processing of omega-3 oils. In: Hernandez E.M., Hosokawa M. (Eds.), *omega-3 oils: Applications in functional foods*. Elsevier Inc., 107–128. DOI: 10.1016/B978-1-893997-82-0.50008-6.

Higham D.J., 2008. Modeling and simulating chemical reactions. *SIAM Rev.*, 50, 347–368. DOI: 10.1137/060666457.

Karacan F., 2015. Steady-state optimization for biodiesel production in a reactive distillation column. *Clean Technol. Environ. Policy*, 17, 1207–1215. DOI: 10.1007/s10098-015-0964-3.

Khan A.K., 2002. *Research into biodiesel kinetics and catalyst development*. PhD thesis. University of Queensland.

Kiss A.A., Bildea, C.S., 2012. A review of biodiesel production by integrated reactive separation technologies. *J. Chem. Technol. Biotechnol.*, 87, 861–879. DOI: 10.1002/jctb.3785.

Levenspiel O., 1999. *Chemical reaction engineering*. 3^{rd} ed. John Wiley & Sons, Inc., New York.

Levenspiel O., Bischoff K.B., 1959. Backmixing in the design of chemical reactors. *Ind. Eng. Chem.*, 51, 1431–1434. DOI: 10.1021/ie50600a023.

Liu R., Wang X., Zhao X., Feng P., 2008. Sulfonated ordered mesoporous carbon for catalytic preparation of biodiesel. *Carbon*, 46, 1664–1669. DOI: 10.1016/j.carbon.2008.07.016.

Machado G.D., Pessoa F.L.P., Castier D., Aranda D.A.G, Ferreira-Pinto L., Giufrida W.M., Cabral V.F., Cardozo-Filho L., 2015. Computer simulation of biodiesel production by hydro-esterification. *XX Congresso Brasileiro de Engenharia Química*, 11119–11126. DOI: 10.5151/chemeng-cobeq2014-0019-27506-160049.

Majeed N.S., Saleh A.A., 2016. Synthesis and characterization of nanocrystalline micro- mesoporous ZSM-5 / MCM-41 Composite Zeolite. *Iraqi J. Chem. Pet. Eng.*, 17 (1), 71–82.

Mann U., 2009. *Principles of chemical reactor analysis and design: New tools for industrial chemical reactor operations*. 2^{nd} ed. John Wiley & Sons, Inc. DOI: 10.1002/9780470385821.

Mod R.R., Magne F.C., Sumrell G., Koos R.E., 1977. Lubricants and lubricant additives: III. Performance characteristics of some thioacetate, phosphorodithioate, and hexachlorocyclopentadiene derivatives of stearic acid amides and esters. *JAOCS*, 54, 589–591. DOI: 10.1007/BF03027643.

Oliveira C.F., Dezaneti L.M., Garcia F.A.C., de Macedo J.L., Dias J.A., Dias S.C.L., Alvim K.S.P., 2010. Esterification of oleic acid with ethanol by 12-tungstophosphoric acid supported on zirconia. *Appl. Catal., A*, 372, 153–161. DOI: 10.1016/j.apcata.2009.10.027.

Prates C.D., Ballotin F.C., Limborço H., Ardisson J.D., Lago R.M., Teixeira A.P. de C., 2020. Heterogeneous acid catalyst based on sulfated iron ore tailing for oleic acid esterification. *Appl. Catal., A*, 600, 117624. DOI: 10.1016/j.apcata.2020.117624.

Raia R.Z., da Silva L.S., Marcucci S.M.P., Arroyo P.A., 2017. Biodiesel production from Jatropha curcas L. oil by simultaneous esterification and transesterification using sulphated zirconia. *Catal. Today,* 289, 105–114. DOI: 10.1016/j.cattod.2016.09.013.

Refaat A.A., 2011. Biodiesel production using solid metal oxide catalysts. *Int. J. Environ. Sci. Technol.,* 8, 203–221. DOI: 10.1007/BF03326210.

Sarkar A., Ghosh S.K., Pramanik P., 2010. Investigation of the catalytic efficiency of a new mesoporous catalyst SnO_2/WO_3 towards oleic acid esterification. *J. Mol. Catal. A: Chem.*, 327, 73–79. DOI: 10.1016/j.molcata.2010.05.015.

Scragg A.H., 2009. *Biofuels: Production, application and development*. CABI Publishing.

Sena S.R.C., Barros Neto E.L., Pereira C.G., 2019. Evaluation of the lubrication of ethyl oleate and ethyl octanoate as gasoline additive. *Braz. J. Pet. Gas*, 13, 111–118. DOI: 10.5419/bjpg2019-0011.

Takagaki A., Toda M., Okamura M., Kondo J.N., Hayashi S., Domen K., Hara M., 2006. Esterification of higher fatty acids by a novel strong solid acid. *Catal. Today,*116, 157–161. DOI: 10.1016/j.cattod.2006.01.037.

Tang J., Liang X., 2015. Highly efficient procedure for biodiesel synthesis using polypyrrole functionalized by sulfonic acid. *Kinet. Catal.*, 56, 323–328. DOI: 10.1134/S002315841503009X.

Tankov I., Yankova R., 2019. DFT analysis, reaction kinetics and mechanism of esterification using pyridinium nitrate as a green catalyst. *J. Mol. Liq.*, 277, 241–253. DOI: 10.1016/j.molliq.2018.12.087.

van Rossum G., 1995. *Python tutorial*. CWI, 1–65.

Vieira S.S., Magriotis Z.M., Graça I., Fernandes A., Ribeiro M.F., Lopes J.M.F.M., Coelho S.M., Santos N.A.V., Saczk A.A., 2017. Production of biodiesel using HZSM-5 zeolites modified with citric acid and SO_4^{2-}/La_2O_3. *Catal. Today*, 279, 267–273. DOI: 10.1016/j.cattod.2016.04.014.

Vieira. S.S., Magriotis Z.M., Filipa M., Graça I., Fernandes A., Manuel J., Lopes F.M., Coelho S.M., Santos Ap. N., V., Saczk Ap.A., 2015. Microporous and mesoporous materials use of HZSM-5 modified with citric acid as acid heterogeneous catalyst for biodiesel production via esterification of oleic acid. *Microporous Mesoporous Mater.*, 201, 160–168. DOI: 10.1016/j.micromeso.2014.09.015.

Yin P., Chen L., Wang Z., Qu R., Liu X., Xu Q., Ren S., 2012. Biodiesel production from esterification of oleic acid over aminophosphonic acid resin D418. *Fuel*, 102, 499–505. DOI: 10.1016/j.fuel.2012.05.027.

Zhou K., Chaemchuen S., 2017. Metal-organic framework as catalyst in esterification of oleic acid for biodiesel production. *Int. J. Environ. Sci. Dev.*, 8, 251–254. DOI: 10.18178/ijesd.2017.8.4.957.

Received 09 October 2020
Received in revised form 04 May 2021
Accepted 05 May 2021